



## Non-hierarchical architected materials with extreme stiffness and strength

Wang, Fengwen; Brøns, Marie; Sigmund, Ole

*Published in:*  
Advanced Functional Materials

*Link to article, DOI:*  
[10.1002/adfm.202211561](https://doi.org/10.1002/adfm.202211561)

*Publication date:*  
2023

*Document Version*  
Peer reviewed version

[Link back to DTU Orbit](#)

*Citation (APA):*  
Wang, F., Brøns, M., & Sigmund, O. (2023). Non-hierarchical architected materials with extreme stiffness and strength. *Advanced Functional Materials*, 33(13), Article 2211561. <https://doi.org/10.1002/adfm.202211561>

---

### General rights

Copyright and moral rights for the publications made accessible in the public portal are retained by the authors and/or other copyright owners and it is a condition of accessing publications that users recognise and abide by the legal requirements associated with these rights.

- Users may download and print one copy of any publication from the public portal for the purpose of private study or research.
- You may not further distribute the material or use it for any profit-making activity or commercial gain
- You may freely distribute the URL identifying the publication in the public portal

If you believe that this document breaches copyright please contact us providing details, and we will remove access to the work immediately and investigate your claim.

# Supporting Information

## Non-hierarchical architected materials with extreme stiffness and strength

Fengwen Wang\* Marie Brøns Ole Sigmund\*

### Hierarchical microstructures

First order hierarchical microstructures ( $P_1$  and  $T_1$ ) possess architected microstructures on level  $n = 1$  and base material on level  $n = 0$ . Second order hierarchical microstructures ( $P_2$  and  $T_2$ ) possess the same architected microstructures on levels  $n = 2$  and  $n = 1$  and base material on level  $n = 0$ . The  $n$ th order hierarchical microstructures possess the same architected microstructures on levels  $n = n, \dots, 1$  and base material on level  $n = 0$ . **Figure S1** illustrates the microstructure configurations of  $P_2$  ((a)) and  $T_2$  ((b)).

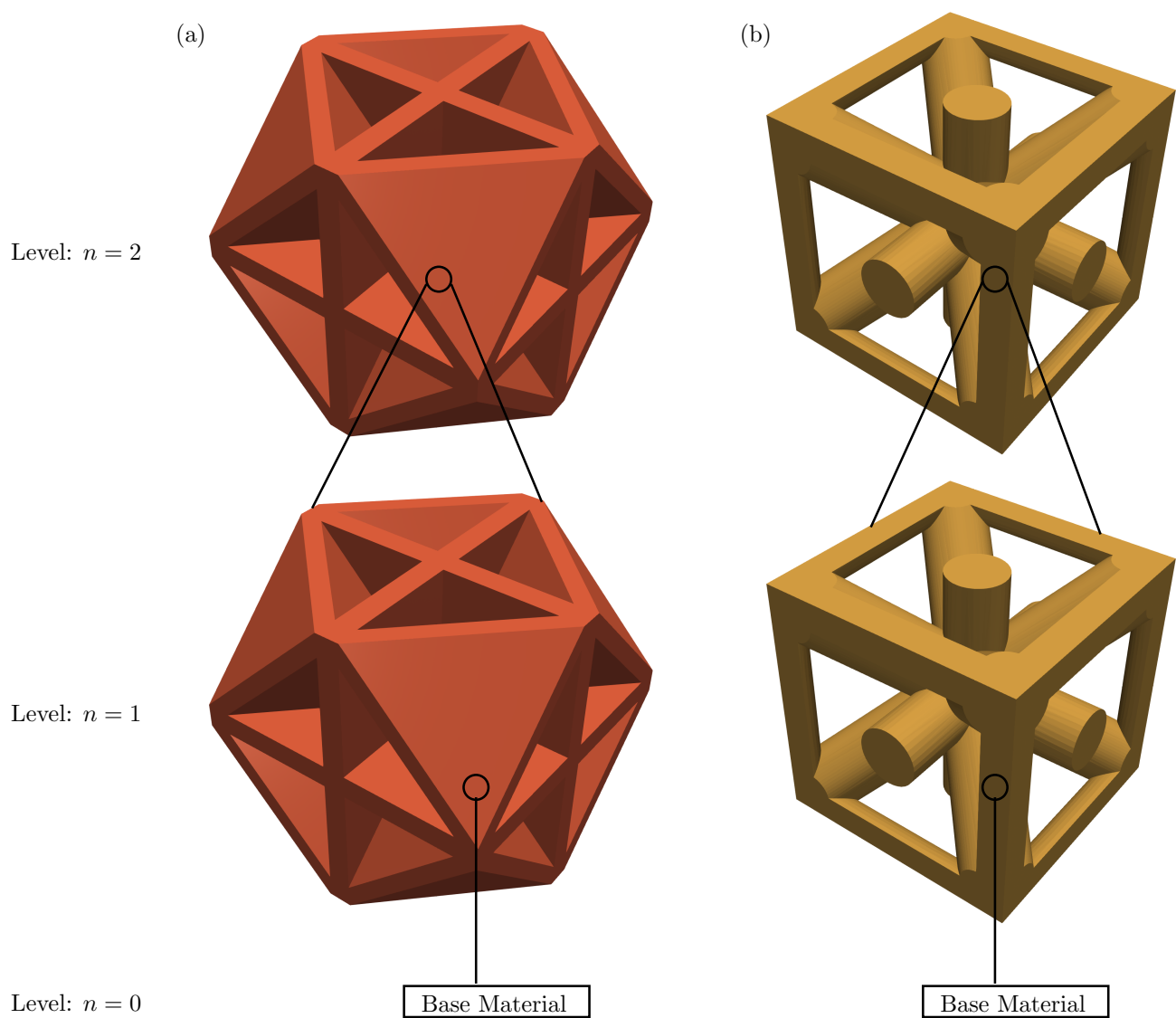


**Figure S1:** Illustration of second order microstructures. (a)  $P_2$ . (b)  $T_2$ .

## Feature-based parameterization of architected materials

To ensure manufacturable open-cell microstructures, a different feature-based parameterization is used here compared to the study in [1], where the feature-based parameterization contains close regions and results in microstructure designs that can not be manufactured.

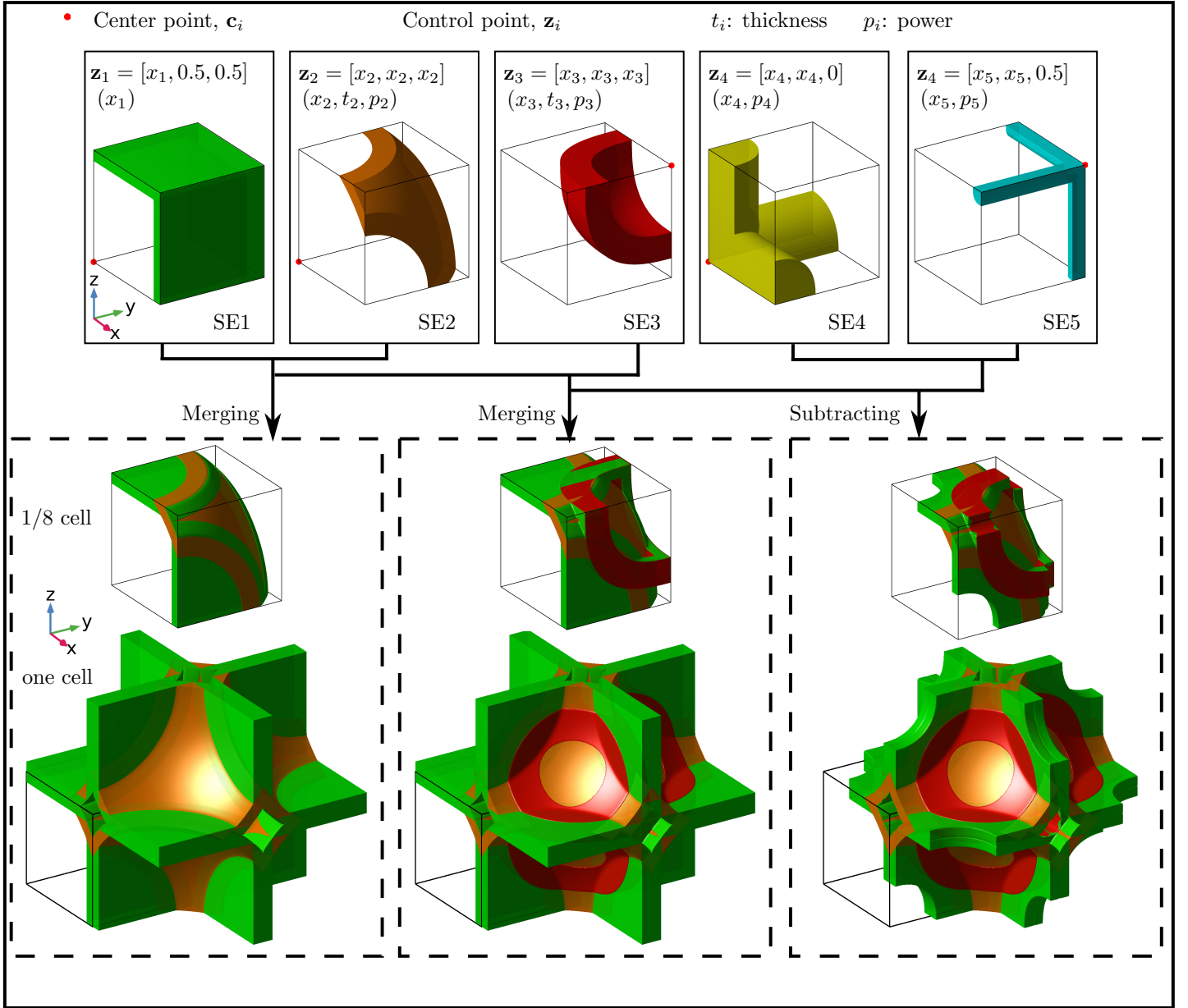


**Figure S2:** Illustration of design parameterization using 1/8 O2 microstructure with symmetry. Top: Features. Bottom: Resulting structures.

In this study, the microstructures are parameterized using five features as illustrated in **Figure S2**, i.e., three hollow super-ellipsoids and two super-ellipsoids to ensure manufacturable open-cell microstructures. **Figure S2** illustrates the feature-based parameterization process using 1/8 O2 microstructure. The  $i$ th hollow super-ellipsoid is controlled by a center point,  $\mathbf{c}_i = [x_{0i}, y_{0i}, z_{0i}]$ , a control point located at the inner super-ellipsoid surface,  $\mathbf{z}_i = [x_{1i}, y_{1i}, z_{1i}]$ , a thickness  $t_i$  and the power  $p_i$ . Each super-ellipsoid is controlled by a center point, a control point, and the power. The center point for SE1, SE2 and SE4 is located at  $[0, 0, 0]$  and the one for SE3 and SE5 is located at  $[0.5, 0.5, 0.5]$ . The center points are highlighted using red dots in **Figure S2**. The control point  $\mathbf{z}_i$  and corresponding design variables are listed together with each feature. It is seen that SE1, SE2 and SE3 together form the microstructure configuration while

SE4 and SE5 are utilized to ensure open cell designs.

Using a fixed grid fictitious domain, densities are employed to represent the relation between the element and the features. The elemental density of  $e$  resulting from the  $i$ th inner and outer super-ellipsoids are defined as,

$$\rho_e^{i,0} = \frac{1}{1 + \exp(\beta_2 H(\mathbf{x}_e, \mathbf{c}_i, \mathbf{z}_i, p_i, 0))}, \quad \rho_e^{i,1} = \frac{1}{1 + \exp(\beta_2 H(\mathbf{x}_e, \mathbf{c}_i, \mathbf{z}_i, p_i, t_i))} \quad (1)$$

where  $\mathbf{x}_e$  is the centroid of element  $e$ ,  $\rho_e^{i,0}$  and  $\rho_e^{i,1}$  denote densities generated by the  $i$ th inner and outer super-ellipsoids, respectively,  $\rho_e^{i,0} = 1$  if  $\mathbf{x}_e$  is inside the  $i$ th inner super-ellipsoid and  $\rho_e^{i,0} = 0$  outside of the  $i$ th inner super-ellipsoid.  $\rho_e^{i,1} = 1$  if  $\mathbf{x}_e$  is inside the  $i$ th outer super-ellipsoid and  $\rho_e^{i,1} = 0$  outside of the  $i$ th outer super-ellipsoid, and  $\beta_2 = 200$  is the projection value, and the  $H$ -operator is defined as

$$H(\mathbf{x}, \mathbf{c}_i, \mathbf{z}_i, p_i, t) = T(\mathbf{x}, \mathbf{c}_i, \mathbf{z}_i, p_i, 0) - T(\mathbf{z}_i, \mathbf{c}_i, \mathbf{z}_i, p_i, t), \quad (2)$$

$$T(\mathbf{x}, \mathbf{c}_i, \mathbf{z}_i, p_i, t) = \sqrt[p_i]{|n_{1i}(x - x_{0i})|^{p_i} + |n_{2i}(y - y_{0i})|^{p_i} + |n_{3i}(z - z_{0i})|^{p_i} + t} \quad (3)$$

where  $\mathbf{x} = [x, y, z]$  represents any given location,  $[n_{1i}, n_{2i}, n_{3i}] = [\mathbf{z}_i - \mathbf{c}_i] / d_i$  is the normalized direction vector between the control and center points, and  $d_i = \|\mathbf{z}_i - \mathbf{c}_i\| + \delta_0$  is the distance between the center point and the control point with  $\delta_0 = 10^{-10}$  to avoid zero denominator.

A final density  $\rho_e$  is introduced to represent the material occupation of the element,  $e$ . The element is occupied by the constitutive base material when  $\rho_e = 1$  and is void when  $\rho_e = 0$ . It is numerically calculated using the density variables generated using the five features, written as

$$\rho_e = (1 - (1 - \rho_e^{1,1} \rho_e^{2,1}) (1 - \rho_e^{3,1} (1 - \rho_e^{3,0}))) (1 - \rho_e^{1,0} \rho_e^{2,0}) (1 - \rho_e^{4,0}) (1 - \rho_e^{5,0}). \quad (4)$$

The intersections between different features are smoothed using filtering. Details can be found in [1].

The optimized parameters for O1, O2 and O3 microstructures are listed in **Table S1** and the corresponding optimized designs are shown in **Figure S3** with isometric and top views.

Design	Parameters for different features				
	SE1 ( $x_1$ )	SE2 ( $x_2, t_2, p_2$ )	SE3 ( $x_3, t_3, p_3$ )	SE4 ( $x_4, p_4$ )	SE5 ( $x_5, p_5$ )
O1	(0.039)	(0.300, 0.038, 1.20)	(0.215, 0.300, 10.00)	(0.060, 4.00)	(0.440, 4.00)
O2	(0.049)	(0.333, 0.034, 1.90)	(0.300, 0.067, 2.76)	(0.144, 2.31)	(0.450, 3.15)
O3	(0.050)	(0.318, 0.031, 2.22)	(0.296, 0.046, 2.06)	(0.141, 2.63)	(0.449, 2.50)

**Table S1:** Feature parameters for O1, O2 and O3 microstructures

## Movie S1

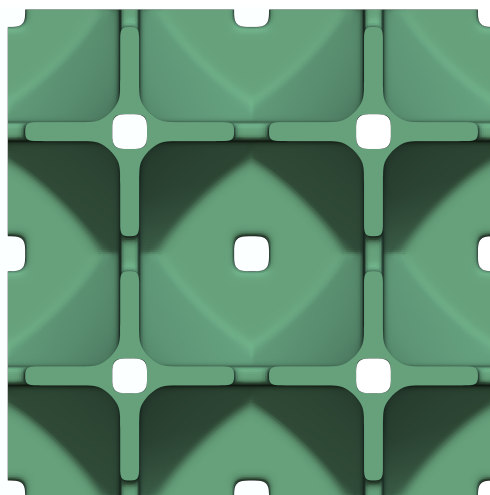
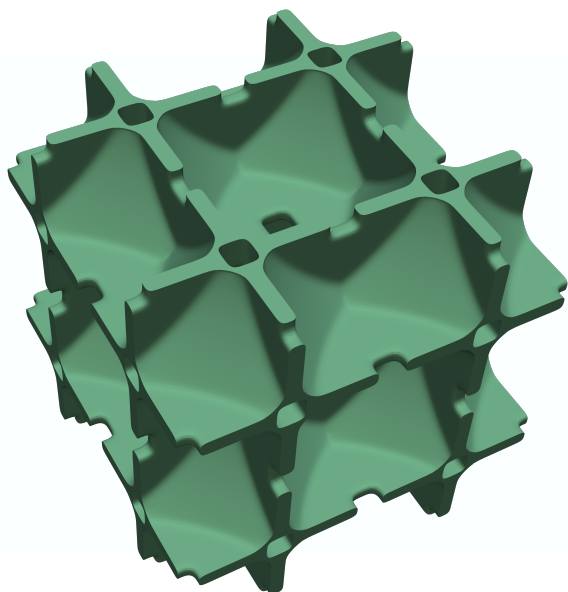
The video shows a typical experiment and is a qualitative supplement visualizing the buckling deformation shape over time.

## References

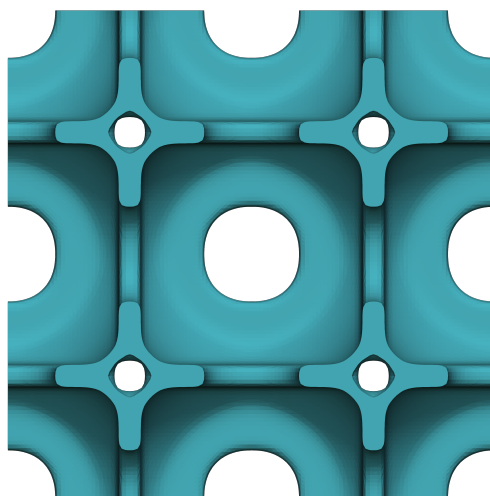
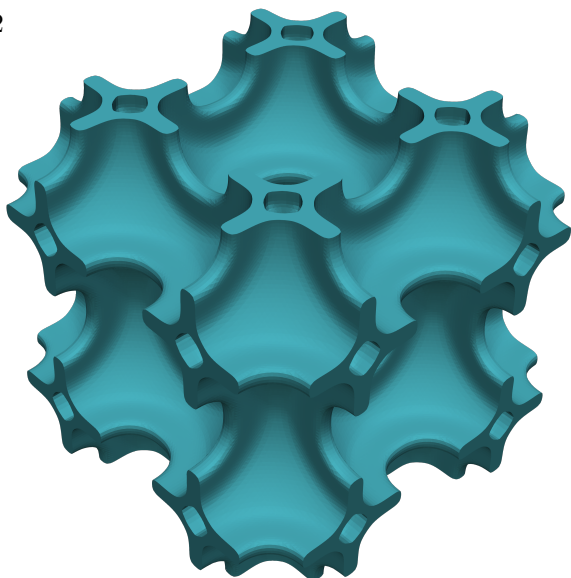
- [1] F. Wang, O. Sigmund, *Journal of the Mechanics and Physics of Solids* **2021**, 152 104415.



O1



O2



O3

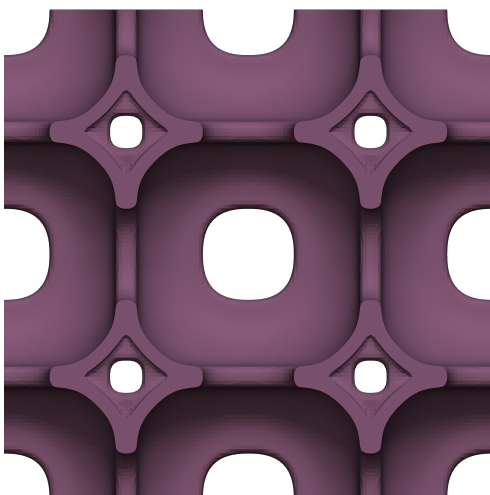
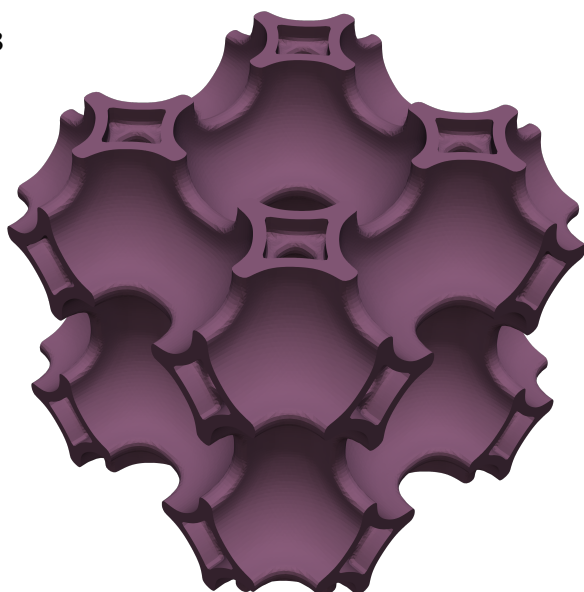


**Figure S3:** Optimized designs for fabrication. Left: Isometric view. Right: Top view